Cell

Cyld Inhibits Tumor Cell Proliferation by Blocking Bcl-3-Dependent NF-κB Signaling

Ramin Massoumi,[1] Katarzyna Chmielarska,[1] Katharina Hennecke,[2] Alexander Pfeifer,[2] and Reinhard Fässler[1,*]
[1] Department of Molecular Medicine, Max Planck Institute of Biochemistry, D-82152 Martinsried, Germany
[2] Molecular Pharmacology, Department of Pharmacy, Ludwig-Maximilians-Universität München, D-81377 Munich, Germany
*Contact: faessler@biochem.mpg.de
DOI 10.1016/j.cell.2006.03.041

SUMMARY

Mutations in the *CYLD* gene cause tumors of hair-follicle keratinocytes. The *CYLD* gene encodes a deubiquitinase that removes lysine 63-linked ubiquitin chains from TRAF2 and inhibits p65/p50 NF-κB activation. Here we show that mice lacking Cyld are highly susceptible to chemically induced skin tumors. $Cyld^{-/-}$ tumors and keratinocytes treated with 12-O-tetradecanoylphorbol-13 acetate (TPA) or UV light are hyperproliferative and have elevated cyclin D1 levels. The cyclin D1 elevation is caused not by increased p65/p50 action but rather by increased nuclear activity of Bcl-3-associated NF-κB p50 and p52. In $Cyld^{+/+}$ keratinocytes, TPA or UV light triggers the translocation of Cyld from the cytoplasm to the perinuclear region, where Cyld binds and deubiquitinates Bcl-3, thereby preventing nuclear accumulation of Bcl-3 and p50/Bcl-3- or p52/Bcl-3-dependent proliferation. These data indicate that, depending on the external signals, Cyld can negatively regulate different NF-κB pathways; inactivation of TRAF2 controls survival and inflammation, while inhibition of Bcl-3 controls proliferation and tumor growth.

INTRODUCTION

Patients with familial cylindromatosis develop multiple, benign tumors of skin appendages (called cylindromas) predominantly in their scalp, neck, and face region (van Balkom and Hennekam, 1994). The cause of cylindroma development is the loss of both *CYLD* alleles (Bignell et al., 2000). CYLD encodes a 107 kDa polypeptide that is ubiquitously expressed and contains a deubiquitinating domain (UCH) at the C terminus, which removes lysine 63 (K63) linked polyubiquitin chains from TNF receptor bound TRAF2 (Trompouki et al., 2003; Brummelkamp et al., 2003; Kovalenko et al., 2003; Regamey et al., 2003). Polyubiquitin chains that are linked through K63 usually serve as docking sites for other proteins, while chains linked through K48 of ubiquitin target proteins to the proteasome for degradation (Pickart 2001; Weissman 2001). The removal of the K63-linked polyubiquitin chain from TRAF2 by CYLD leads to the inhibition of the IκB kinase (IKK) complex, stabilization of the NF-κB inhibitor IκB-α, and retention of the classic NF-κB heterodimer p65/p50 in the cytoplasm. Hence, it was postulated that mutations in the *CYLD* gene cause hyperactivation of p65/p50 NF-κB, leading to tumor cell survival and the formation of cylindromas (Trompouki et al., 2003; Brummelkamp et al., 2003; Kovalenko et al., 2003). In contrast to this hypothesis, however, it has been shown that transgenic overexpression of constitutively nuclear p50 and p65 NF-κB in keratinocytes of mice results in epidermal hypoplasia and growth inhibition rather than epidermal hyperplasia (Seitz et al., 1998). Thus, it is not fully understood how loss of CYLD induces the formation of cylindromas and whether increased NF-κB signaling plays a role in skin tumor formation.

The NF-κB family consists of five members called p65 (RelA), RelB, c-Rel, p50/p105 (NF-κB1), and p52/p100 (NF-κB2). They regulate a broad spectrum of physiological and pathophysiological processes such as inflammation, immune response, cell survival, and cell proliferation (Ghosh and Karin, 2002). While p65 (RelA), RelB, and c-Rel are synthesized as mature proteins associated with inhibitory factor IκB protein, p50 and p52 are first synthesized as large precursors termed p105 and p100, respectively. A variety of signals can release cytoplasmic retention and trigger the nuclear translocation of NF-κB through induced degradation of either IκB proteins (canonical NF-κB pathway) or IκB-homologous regions in the C terminus of p105 and p100 (alternative NF-κB pathway). RelB, c-Rel, and p65 (RelA) contain a DNA binding domain (called Rel homology domain) through which they interact with NF-κB binding sites of target genes and a transactivation domain through which they activate transcription (Ghosh and Karin, 2002; Israel, 2000). In contrast, p50 and p52 have only a DNA binding domain and lack a transactivation domain. Therefore, p50 and p52

are only able to promote gene transcription if they either form a heterodimer with p65 (RelA), RelB, or c-Rel or recruit the coactivator Bcl-3, which contains a transactivation domain that switches the transcriptional properties of NF-κB p50 or p52 homodimers from a repressive to an activating state (Watanabe et al., 1997; Fujita et al., 1993).

Bcl-3 was originally identified in a subgroup of B cell leukemias that carry a translocation of the immunoglobulin heavy chain (IgH) promoter adjacent to the Bcl-3 coding region (McKeithan, et al., 1990). Subsequently, it was demonstrated that Bcl-3 associates with the NF-κB p50 or p52 subunits and strongly enhances cell proliferation and oncogenesis through activation of the *cyclin D1* promoter (Westerheide et al., 2001, Rocha et al., 2003). In B and T cells, as well as in transiently transfected cells, Bcl-3 exhibited predominantly nuclear localization (Nishikori et al., 2003; Zhang et al., 1994; Nolan et al., 1993; Bours et al., 1993), while in several other cell types such as erythroblasts or hepatocytes, Bcl-3 resides in the cytoplasm and requires activation prior to nuclear translocation (Zhang et al., 1998; Brasier et al., 2001). The signals that activate Bcl-3 and recruit Bcl-3 to the NF-κB p50 and p52 subunits in the nucleus are not known.

Here we show that mice lacking Cyld are prone to chemically induced skin tumors. Our data indicate that Cyld inhibits tumor formation and keratinocyte proliferation by removing K63-linked polyubiquitin chains from Bcl-3, which results in retention of Bcl-3 in the cytoplasm. In Cyld-deficient keratinocytes, Bcl-3 accumulates in the nucleus, activates the NF-κB subunits p50 and p52, and induces the transcription of NF-κB target genes such as the *cyclin D1* gene.

RESULTS

Cyld$^{-/-}$ Mice Are Highly Sensitive to Skin Tumor Development

To explore the function of Cyld in vivo, we generated Cyld-deficient mice by inserting a *lacZ* reporter gene into the ATG-encoding exon 4 (see Figure S1 in the Supplemental Data available with this article online). We confirmed the absence of *Cyld* mRNA and protein in cells and tissues from *Cyld*$^{-/-}$ mice by Western blot and RT-PCR analyses (Figure 1A and Figure S1). *Cyld*$^{-/-}$ mice had no apparent phenotype, even in the skin epithelium, where Cyld is prominently expressed (Figures 1A and 1B). Moreover, *Cyld*$^{-/-}$ mice displayed normal numbers of proliferating keratinocytes in the basal layers of the epidermis and in the hair matrix (data not shown). Furthermore, they were fertile, had a normal life span, and did not spontaneously develop tumors.

To assess the tumor suppressor function of Cyld in vivo, we induced skin tumors by treating *Cyld*$^{-/-}$ mice and littermate controls with a single initiation dose of 7,12-dimethylbenz(a)anthracene (DMBA) followed by 12-O-tetradecanoylphorbol-13 acetate (TPA) twice per week. After a latency period of 7–11 weeks, all *Cyld*$^{-/-}$ mice developed tumors, whereas only 50% of *Cyld*$^{+/+}$ mice developed papillomas after 11–16 weeks (Figure 1C and Figure 2A). Induced *Cyld*$^{-/-}$ mice also developed 7-fold more and significantly larger papillomas than control littermates (Figures 2B and 2C). Interestingly, tumor frequency and growth of tumors in *Cyld*$^{+/-}$ mice was intermediate between that of *Cyld*$^{+/+}$ and *Cyld*$^{-/-}$ (Figure 1C and Figures 2A–2C), indicating that *Cyld* gene dosage plays a critical role in DMBA/TPA-induced tumor development. We analyzed all tumors of both groups of mice histologically and observed a hyperplastic squamous epithelium and no signs of malignancy in both *Cyld*$^{-/-}$ as well as *Cyld*$^{+/+}$ tumors (Figure 1D). Immunostaining of tumor sections revealed that papillomas from control littermates expressed high levels of Cyld, whereas Cyld was absent in *Cyld*$^{-/-}$ tumors (Figure 1E).

The loss of Cyld leads to increased susceptibility to chemically induced skin tumor formation, confirming that Cyld functions as a tumor suppressor in skin. To determine whether *Cyld* deficiency affects DMBA-induced tumor initiation or TPA-induced tumor promotion, we treated control and *Cyld*$^{-/-}$ mice repeatedly with DMBA alone. This treatment predominantly induces squamous cell carcinomas (Quintanilla et al., 1986) and gave rise to tumors with similar size and number in all *Cyld*$^{-/-}$ and *Cyld*$^{+/+}$ mice (Figures 2D–2F). This finding strongly suggests that Cyld is required to suppress TPA-induced tumor promotion but not DMBA-induced tumor initiation.

Cyld Regulates Proliferation and Cyclin D1 Expression in a NF-κB-Dependent Manner

The increased tumor formation in DMBA/TPA-treated *Cyld*$^{-/-}$ mice could be due to increased keratinocyte survival and/or proliferation. To determine the extent of apoptosis in *Cyld*$^{+/+}$ and *Cyld*$^{-/-}$ tumors, we performed TUNEL staining and immunostaining of cleaved caspase-3. These experiments revealed that 1.0% and 1.1% of the keratinocytes were apoptotic in *Cyld*$^{+/+}$ and *Cyld*$^{-/-}$ tumor sections, respectively, and thus indicated that loss of Cyld does not grossly affect tumor cell survival. To examine cell proliferation, we compared BrdU incorporation and Ki67 and cyclin D1 expression between *Cyld*$^{-/-}$ and *Cyld*$^{+/+}$ tumors. *Cyld*$^{-/-}$ tumors displayed a significant increase in Ki67- and cyclin D1-positive cells in the basal cell layers (Figure 3A and Figure S2). Moreover, *Cyld*$^{-/-}$ tumors contained large numbers of proliferating cells above the basal cell layer, which were never observed in *Cyld*$^{+/+}$ tumors (Figure 3A). These data suggest that TPA increases tumor promotion in *Cyld*$^{-/-}$ mice by enhancing tumor cell proliferation. Therefore, we tested whether treatment with TPA alone was sufficient to induce skin tumors in *Cyld*$^{-/-}$ mice. The application of a single dose of TPA was already sufficient to induce epidermal hyperplasia and to dramatically increase keratinocyte proliferation on the back skin of *Cyld*$^{-/-}$ mice (Figure 3B). However, we never observed the formation of skin tumors in *Cyld*$^{-/-}$ mice, even after a prolonged TPA treatment for 20 weeks. Altogether, these findings indicate that loss of Cyld leads to increased TPA-induced tumor cell proliferation and,

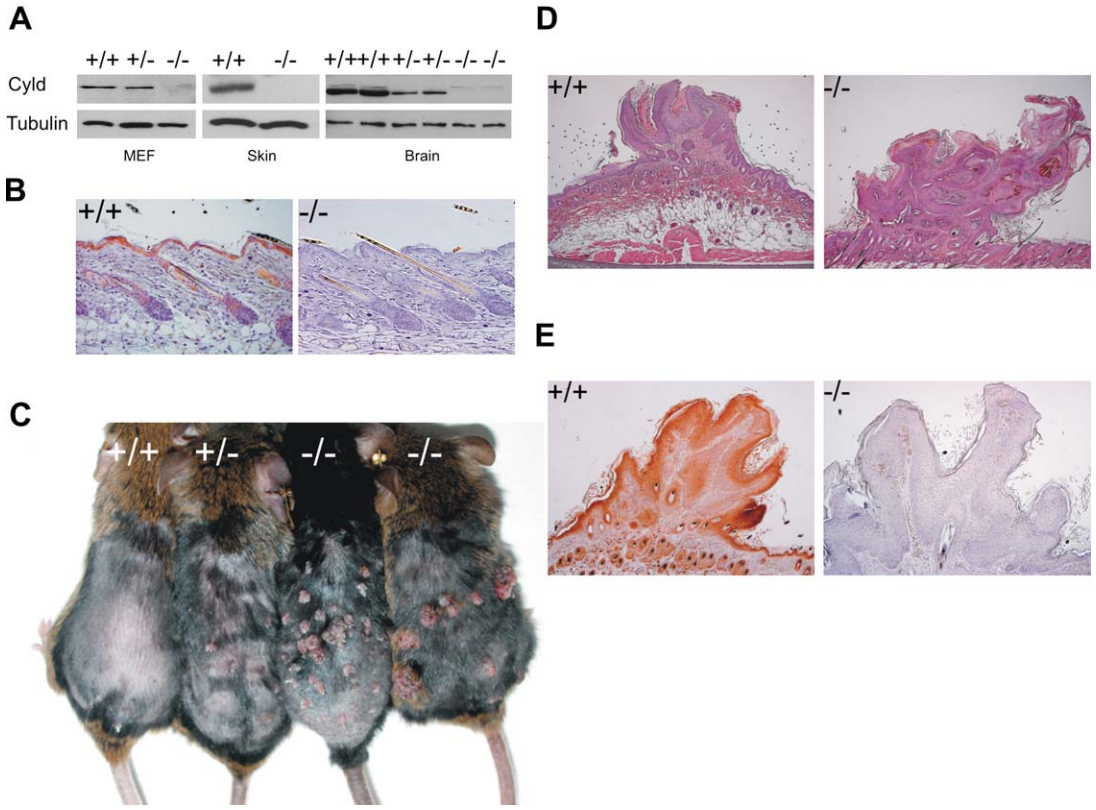

Figure 1. Analysis of the Role of Cyld in Papilloma Formation

(A) Mouse embryonic fibroblast (MEF), skin, and brain protein extracts from *Cyld*$^{+/+}$, *Cyld*$^{+/-}$, and *Cyld*$^{-/-}$ mice probed with a Cyld-specific antibody.

(B) Histological analysis of Cyld expression (red staining) in skin of *Cyld*$^{+/+}$ and *Cyld*$^{-/-}$ mice.

(C) Representative examples of papilloma development in *Cyld*$^{+/+}$, *Cyld*$^{+/-}$, and *Cyld*$^{-/-}$ mice (n = 15) after 16 weeks of DMBA/TPA treatment.

(D) Hematoxylin-and-eosin staining of papillomas of *Cyld*$^{+/+}$ and *Cyld*$^{-/-}$ mice after 16 weeks of DMBA/TPA treatment.

(E) Cyld immunostaining (brown) of papilloma from a *Cyld*$^{+/+}$ and *Cyld*$^{-/-}$ mouse.

together with additional mutations, to the formation of skin tumors in *Cyld*$^{-/-}$ mice.

We then examined whether the TPA-induced proliferation and cyclin D1 expression is also significantly increased in isolated primary *Cyld*$^{-/-}$ keratinocytes. The basal proliferation rate and cyclin D1 expression level did not differ significantly between *Cyld*$^{-/-}$ and *Cyld*$^{+/+}$ keratinocytes (Figures 3C and 3D). However, TPA treatment significantly stimulated the proliferation of *Cyld*$^{-/-}$, but not *Cyld*$^{+/+}$, keratinocytes after 48 hr (Figure 3C) and induced a strong and progressive increase of cyclin D1 expression in *Cyld*$^{-/-}$ keratinocytes, while cyclin D1 levels in *Cyld*$^{+/+}$ keratinocytes decreased 12 hr after TPA treatment (Figure 3D).

Cylindromas develop in the face, neck, and scalp region (van Balkom and Hennekam, 1994), and therefore UV light is considered, at least in part, to trigger tumor growth. Indeed, when we treated primary keratinocytes with a single dose of UV-B, the proliferation rate as well as cyclin D1 expression increased significantly in *Cyld*$^{-/-}$ keratinocytes (Figure S3 and data not shown). In contrast to TPA or UV-B treatment, TNF-α inhibited proliferation of both *Cyld*$^{+/+}$ and *Cyld*$^{-/-}$ keratinocytes and failed to upregulate cyclin D1 expression in *Cyld*$^{-/-}$ keratinocytes (Figure 3C and data not shown). Based on these findings, we conclude that TPA or UV-B light, but not TNF-α, induces cyclin D1 expression and cell proliferation in keratinocytes and that this response is negatively regulated by Cyld.

Cyclin D1 expression can be induced through the activation of various signaling proteins, including protein kinase B (PKB/Akt), mitogen-activated protein kinase (p38 MAPK), c-Jun NH_2-terminal kinase (JNK), and NF-κB (Liang and Slingerland, 2003; Wilkinson and Millar, 2000; Guttridge et al., 1999; Hinz and Strauss, 1999). To test whether TPA treatment induced phosphorylation of JNK, p38 MAPK, and Akt, we isolated primary keratinocytes and monitored the activity of these signaling molecules with specific phosphoantibodies. The phosphorylation of JNK, p38 MAPK, and Akt was comparable in serum-starved *Cyld*$^{+/+}$ and *Cyld*$^{-/-}$ keratinocytes and could be induced by TPA in *Cyld*$^{-/-}$ keratinocytes to an extent similar to in *Cyld*$^{+/+}$ keratinocytes (Figure S4), indicating that these signaling proteins are unlikely to play a major role in the upregulation of cyclin D1.

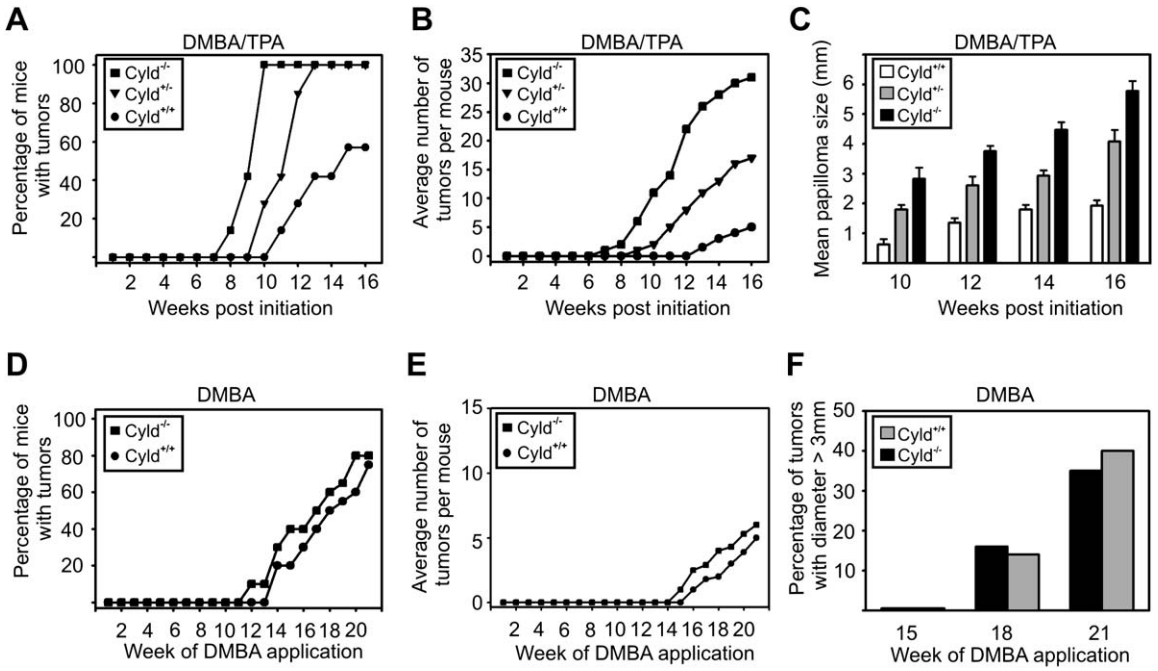

Figure 2. Tumor Development in *Cyld*$^{-/-}$ Mice

(A–C) Tumor incidence (A), average number of tumors per mouse (B), and tumor growth (C) are significantly different between *Cyld*$^{+/+}$ and *Cyld*$^{-/-}$ mice (n = 15; $p < 0.01$).

(D–F) Tumor growth after DMBA treatment alone for 21 weeks is not significantly different between *Cyld*$^{+/+}$ and *Cyld*$^{-/-}$ mice (n = 10).

The *cyclin D1* promoter contains specific NF-κB binding sites and robustly responds to activated NF-κB proteins in several cell lines (Joyce et al., 2001). To examine whether Cyld increases cyclin D1 expression in keratinocytes through activation of NF-κB, we compared the activity of wild-type and NF-κB binding-deficient *cyclin D1* (*Mut-CD1*) promoter-driven luciferase constructs in *Cyld*$^{+/+}$ and *Cyld*$^{-/-}$ keratinocytes. TPA or UV-B treatment increased *cyclin D1* promoter activity significantly more in *Cyld*$^{-/-}$ keratinocytes than in *Cyld*$^{+/+}$ keratinocytes (Figure 3E and Figure S5). The increased *cyclin D1* activation in *Cyld*$^{-/-}$ keratinocytes was normalized upon reintroduction of the Cyld protein (Figure 3E). Importantly, TPA or UV-B failed to activate the *Mut-CD1* promoter in *Cyld*$^{+/+}$ as well as *Cyld*$^{-/-}$ keratinocytes (Figure 3E and Figure S5), indicating that Cyld modulates TPA- or UV-B-mediated *cyclin D1* promoter activation in an NF-κB-dependent manner. TNF-α treatment failed to activate the *cyclin D1* promoter in *Cyld*$^{+/+}$ as well as *Cyld*$^{-/-}$ keratinocytes (Figure 3E), consistent with the inability of TNF-α to stimulate keratinocyte proliferation (Figure 3C). Based on these data, we conclude that TPA and UV light induce the activation of the *cyclin D1* promoter through NF-κB signals that are antagonized by Cyld.

TPA and UV Light Trigger the Activation of Bcl-3/p50 and Bcl-3/p52 in *Cyld*$^{-/-}$ Keratinocytes

The mammalian NF-κB family of transcription factors consists of five members, p65/RelA, c-Rel, RelB, NF-κB1/p50, and NF-κB2/p52, which bind to the NF-κB DNA binding sites as homo- or heterodimers (Ghosh and Karin, 2002; Israel, 2000). Cyld has been implicated in the inhibition of p65/p50 NF-κB through deubiquitination of TRAF2 and subsequent stabilization of IκB-α (Trompouki et al., 2003; Brummelkamp et al., 2003; Kovalenko et al., 2003). Hence, *Cyld*$^{-/-}$ keratinocytes should exhibit increased p65/p50 activity. To test this hypothesis, we treated keratinocytes with TNF-α and monitored both the IκB-α levels and the activity of the p65/p50 NF-κB-responsive 3XκB luciferase reporter (3XκB) construct (Figure 4A). These experiments showed that TNF-α decreased IκB-α levels more rapidly in *Cyld*$^{-/-}$ than in *Cyld*$^{+/+}$ keratinocytes (Figure 4A) and led to a significantly higher activation of the 3XκB luciferase reporter (3XκB) construct in primary *Cyld*$^{-/-}$ keratinocytes compared to *Cyld*$^{+/+}$ keratinocytes (Figure 4B). Moreover, transfection of p65 alone or in combination with p50 increased the 3XκB luciferase reporter activity to a similar extent in *Cyld*$^{+/+}$ and *Cyld*$^{-/-}$ keratinocytes (Figure 4C), confirming that Cyld negatively regulates p65/p50 NF-κB activity upstream of the IκB/NF-κB complex. Surprisingly, however, TPA treatment failed to induce IKK-mediated phosphorylation of IκB-α and phosphorylation-induced degradation of IκB-α in *Cyld*$^{+/+}$ as well as in *Cyld*$^{-/-}$ keratinocytes (Figures 4D and 4E and Figure S6). These results indicate that TPA triggers activation of NF-κB—unlike TNF-α—in an IκB-α-independent manner in keratinocytes.

To address which NF-κB family member (or members) regulates (or regulate) *cyclin D1* promoter activity in

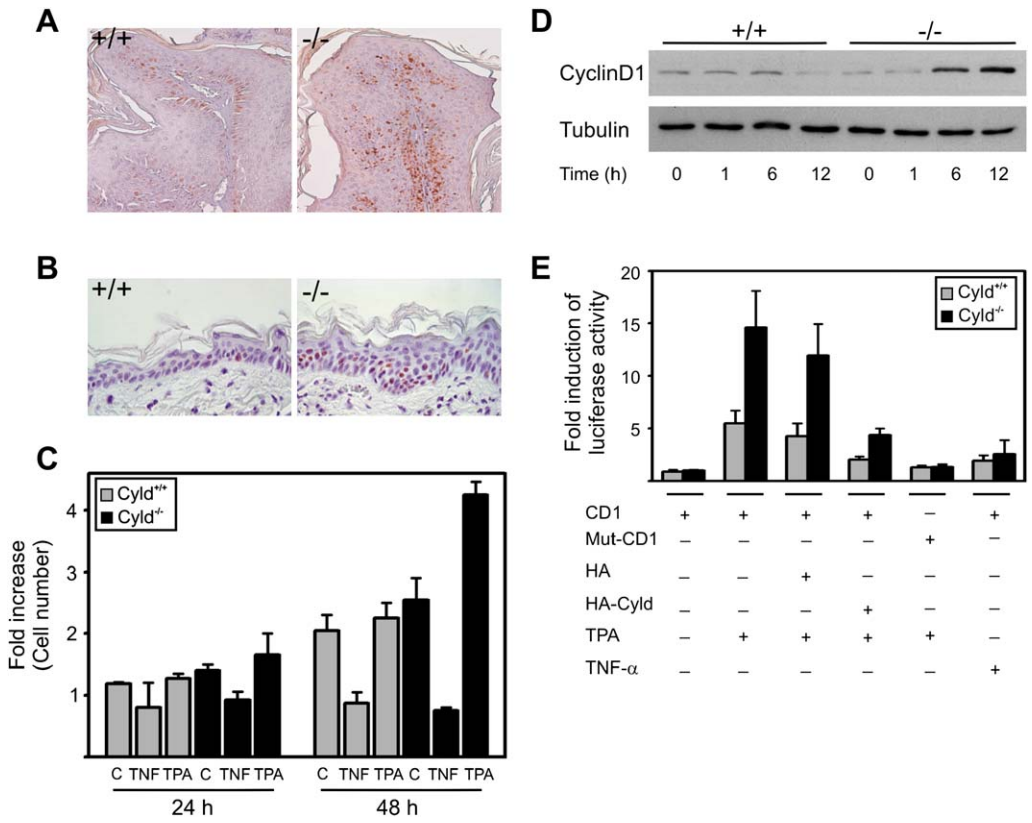

Figure 3. Cell Proliferation in the Absence of Cyld

(A) Ki67 (brown) staining in *Cyld*$^{+/+}$ and *Cyld*$^{-/-}$ tumors after application of DMBA/TPA.

(B) Cyclin D1 staining (brown) in skin 72 hr after a single application of TPA.

(C) Proliferation assay with isolated primary epidermal keratinocytes in the absence or presence of TNF-α (25 ng/ml) or TPA (100 nM). The proliferation rate after 48 hr is significantly higher in *Cyld*$^{-/-}$ compared to *Cyld*$^{+/+}$ in the presence of TPA ($n = 4$; $p < 0.05$).

(D) Analysis of the expression levels of cyclin D1 after treatment with 100 nM TPA as indicated in *Cyld*$^{+/+}$ and *Cyld*$^{-/-}$ keratinocytes.

(E) Activation of the −64 to +10 *cyclin D1* promoter luciferase reporter construct with (CD1) or without (Mut-CD1) the NF-κB site in *Cyld*$^{+/+}$ and *Cyld*$^{-/-}$ keratinocytes in the absence or presence of TPA (100 nM; 2 hr) or TNF-α (25 ng/ml; 2 hr). The *cyclin D1* activity is significantly higher in TPA-treated *Cyld*$^{-/-}$ keratinocytes compared to *Cyld*$^{+/+}$ keratinocytes ($n = 6$; $p < 0.05$).

a Cyld-dependent manner, we transiently transfected *Cyld*$^{+/+}$ and *Cyld*$^{-/-}$ keratinocytes with the *cyclin D1* promoter luciferase construct and expression vectors encoding p65, p50, p52, and Bcl-3 proteins alone or in combination. The proteins p50 and p52 are the final products of the proteasome-mediated processing of two larger precursors, p100 and p105, respectively, which lack transactivation domains (Ghosh and Karin, 2002; Israel, 2000). Therefore, p50 and p52 depend on the association with the noninhibitory IκB family member Bcl-3 (Watanabe et al., 1997; Fujita et al., 1993; Westerheide et al., 2001; Rocha et al., 2003). Expression of the NF-κB subunits p50, p52, p65, or p65 and p50 together significantly increased *cyclin D1* promoter activity in neither *Cyld*$^{+/+}$ nor *Cyld*$^{-/-}$ keratinocytes (Figure 4F). Similarly, addition of Bcl-3 alone failed to increase cyclin D1 in *Cyld*$^{+/+}$ and *Cyld*$^{-/-}$ keratinocytes. However, Bcl-3 in combination with p50 or p52 strongly activated the *cyclin D1* promoter. This effect was significantly more pronounced in *Cyld*$^{-/-}$ keratinocytes than in *Cyld*$^{+/+}$ cells (Figure 4F). Importantly, the increased *cyclin D1* promoter activity in *Cyld*$^{-/-}$ keratinocytes was normalized after re-expression of Cyld and completely abolished in the absence of a functional NF-κB binding site (Figure 4G). Based on these data, we conclude that loss of Cyld in keratinocytes does not promote the activity of the p65/p50 NF-κB but rather promotes the synergistic activation of p50/Bcl-3 or p52/Bcl-3, leading to increased expression of NF-κB-dependent genes, including *cyclin D1*.

Cyld Regulates Nuclear Accumulation of Bcl-3 in Keratinocytes

To unravel the mechanism underlying the inhibitory activity of Cyld on TPA-mediated p50/Bcl-3 or p52/Bcl-3, we first determined the subcellular localization of Cyld and Bcl-3 in keratinocytes. Expression of an EGFP-tagged Cyld in *Cyld*$^{-/-}$ keratinocytes revealed a cytoplasmic distribution (Figure 5A). Within 30 min after TPA or UV-B treatment, Cyld translocated to and accumulated at the

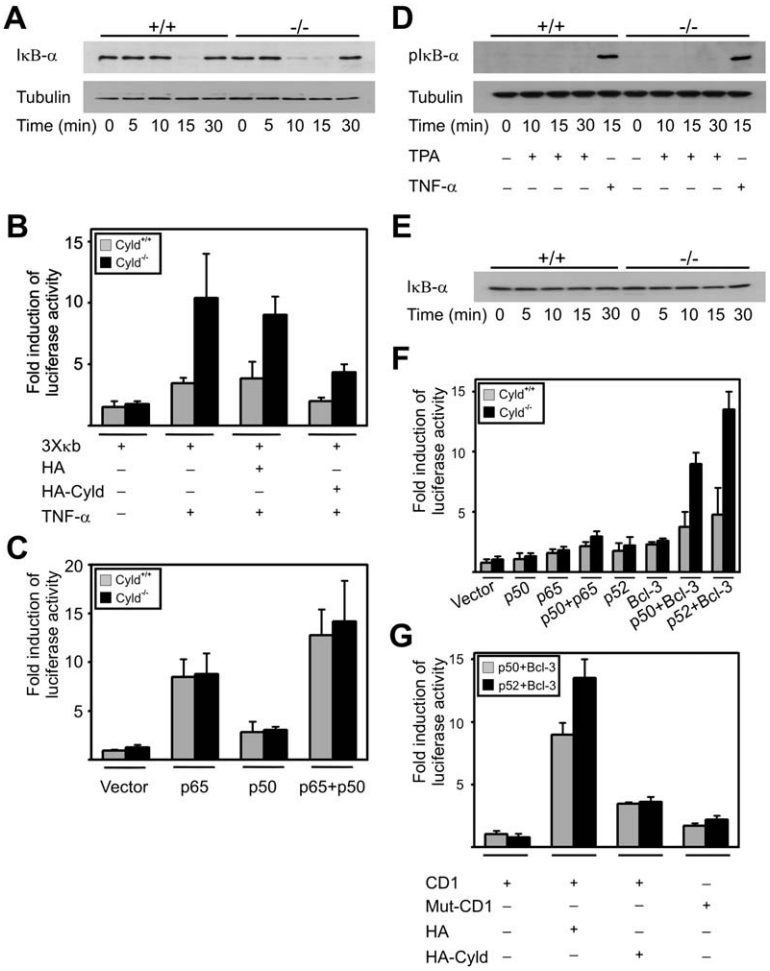

Figure 4. NF-κB-Dependent 3XκB Luciferase Reporter Activity

(A) IκB-α expression level after stimulation with TNF-α in *Cyld*$^{+/+}$ and *Cyld*$^{-/-}$ keratinocytes.

(B) Activation of 3XκB luciferase reporter construct in *Cyld*$^{+/+}$ and *Cyld*$^{-/-}$ keratinocytes in the absence or presence of TNF-α (25 ng/ml; 2 hr) and expression vectors encoding the HA tag or the HA-tagged Cyld.

(C) 3XκB luciferase reporter activity in *Cyld*$^{+/+}$ and *Cyld*$^{-/-}$ keratinocytes transfected with expression plasmids encoding p50 or p65 alone or in combination as indicated.

(D) Phospho-IκB-α (pIκB-α) expression level after stimulation with TPA or TNF-α in *Cyld*$^{+/+}$ and *Cyld*$^{-/-}$ keratinocytes.

(E) IκB-α expression level after stimulation with TPA in *Cyld*$^{+/+}$ and *Cyld*$^{-/-}$ keratinocytes.

(F) *Cyclin D1* promoter activity is significantly increased in *Cyld*$^{-/-}$ keratinocytes upon expression of p50/Bcl-3 or p52/Bcl-3 ($n = 5$; $p < 0.05$).

(G) *Cyld*$^{-/-}$ keratinocytes were cotransfected with the −64 to +10 *cyclin D1* promoter luciferase construct with (CD1) or without (Mut-CD1) the κB site and expression vectors encoding the HA tag or the HA-tagged Cyld alone or in combination, plus p50 or p52 and Bcl-3, as indicated.

perinuclear region, where it colocalized with Bcl-3 (Figures 5A and 5B and Figure S8). The perinuclear accumulation of Cyld was not due to changes in cell shape because F-actin staining of TPA-treated keratinocytes revealed normal cell spreading (Figure 5A).

The colocalization of Cyld and Bcl-3 in the perinuclear region of TPA- or UV-B-treated keratinocytes suggested that Cyld may associate with Bcl-3 and regulate its activity. Coimmunoprecipitation experiments in primary keratinocytes revealed that TPA facilitated the association of endogenous Cyld with endogenous Bcl-3 already 15 min after TPA treatment (Figure 5C). To examine whether the interaction between Cyld and Bcl-3 is achieved through a direct or an indirect interaction, we performed yeast two-hybrid assays. These assays revealed that full length Bcl-3 indeed interacted with Cyld and that the binding site for Bcl-3 on Cyld corresponded to the C-terminal part of the protein (Figures 5D and S7). The consequences of this interaction for the subcellular localization of Bcl-3 were further tested in TPA- as well as UV-B-treated keratinocytes. Either treatment increased nuclear translocation of Bcl-3 significantly more in *Cyld*$^{-/-}$ than in *Cyld*$^{+/+}$ keratinocytes (Figures 5E and 5G and Figures S8), while the level of cytoplasmic Bcl-3 decreased concomitantly in *Cyld*$^{-/-}$ but not *Cyld*$^{+/+}$ keratinocytes (Figure 5F). Importantly, nuclear accumulation of Bcl-3 was also significantly increased in DMBA/TPA-induced *Cyld*$^{-/-}$ tumors when compared with tumors from control littermates (Figure 5H). Moreover, immunostaining revealed increased nuclear staining of Bcl-3 in tumor cells from human cylindromas (Figure 5H), whereas in both normal human and murine epidermal keratinocytes, Bcl-3 was localized in the cytoplasm (Figures 5H and 5I). These findings indicate that Bcl-3 is regulated similarly in human cylindromas, as well as in DMBA/TPA-induced murine skin tumors.

The nuclear accumulation of Bcl-3 and the increased expression of cyclin D1 in tumors and TPA-treated keratinocytes from *Cyld*$^{-/-}$ mice suggest that Bcl-3 becomes directly bound to the NF-κB binding site of the *cyclin D1* promoter to switch on p50 and p52 activity in *Cyld*$^{-/-}$ cells. To test this hypothesis, we performed chromatin immunoprecipitation (ChIP) experiments with anti-Bcl-3 antibodies and semiquantitative PCR amplification of immunoprecipitated chromatin fragments flanking the NF-κB binding site in the *cyclin D1* gene. The ChIP experiments

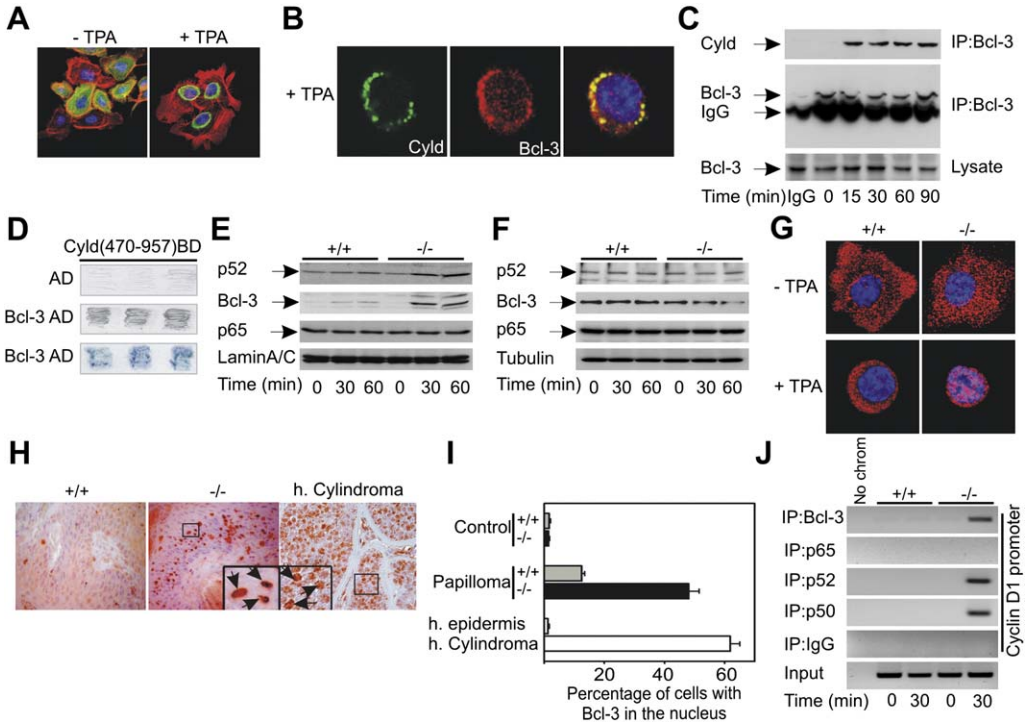

Figure 5. Effects of TPA on the Subcellular Localization of Cyld and Bcl-3

(A) Confocal plane of untreated and TPA-treated (30 min) *Cyld*$^{-/-}$ keratinocytes stably transfected with EGFP-Cyld (green) and stained for F-actin (red) and DAPI (blue).

(B) *Cyld*$^{-/-}$ keratinocytes stably expressing EGFP-Cyld (green) were stimulated with TPA for 30 min and stained for Bcl-3 (red) and DAPI (blue).

(C) *Cyld*$^{+/+}$ keratinocytes were stimulated with TPA for the indicated time periods, lysed, immunoprecipitated with an anti-Bcl-3 antibody, and then probed with an anti-Cyld antibody (upper panel). The blot was reprobed with an anti-Bcl-3 antibody (middle panel). Lysate (lower panel) shows equal amount of Bcl-3 used for immunoprecipitation.

(D) Specific interaction of Cyld and Bcl-3 in yeast. Growth on selective medium of yeast cotransfected with AD (empty vector) and Cyld (470–957) BD (upper panel) or Bcl-3 AD and Cyld (470–957) BD (middle panel). Specific β-galactosidase activity for Cyld (470–957) BD and Bcl-3 AD colonies is shown in the bottom panel.

(E) *Cyld*$^{+/+}$ and *Cyld*$^{-/-}$ keratinocytes were treated with TPA, and nuclear extracts were prepared and immunoblotted with antibodies against p52, p65, Bcl-3, and laminA/C.

(F) *Cyld*$^{+/+}$ and *Cyld*$^{-/-}$ keratinocytes were treated with TPA, and the cytoplasmic fraction was purified and immunoblotted with antibodies against p52, p65, Bcl-3, and tubulin.

(G) Confocal plane of untreated and TPA-treated (30 min) *Cyld*$^{+/+}$ and *Cyld*$^{-/-}$ keratinocytes stained for Bcl-3 (red) and DAPI (blue).

(H) Bcl-3 (brown) staining in *Cyld*$^{+/+}$ and *Cyld*$^{-/-}$ tumors and human cylindromas. The arrows (insert) indicate nuclear localization of Bcl-3.

(I) Percentage of cells with nuclear staining of Bcl-3 in *Cyld*$^{+/+}$ and *Cyld*$^{-/-}$ interfollicular epidermis or DMBA/TPA induced tumors versus human interfollicular epidermis and cylindromas.

(J) Recruitment of Bcl-3, p65, p52, and p50 to the *cyclin D1* promoter by ChIP using untreated or TPA-stimulated (30 min) primary keratinocytes. IP:Bcl-3, IP:p65, IP:p52, and IP:p50, immunoprecipitation (IP) using polyclonal antibodies as indicated; IP:IgG, IP using preimmune serum; input, 10% of the cell lysate used for the IP is shown.

clearly demonstrated that no DNA bound Bcl-3 was detected in resting *Cyld*$^{+/+}$ and *Cyld*$^{-/-}$ keratinocytes. TPA treatment, however, resulted in Bcl-3 binding to endogenous cyclin D1 sequences in *Cyld*$^{-/-}$ keratinocytes, but not in *Cyld*$^{+/+}$ keratinocytes (Figure 5J). Interestingly, TPA also triggered the recruitment of p50 or p52, but not p65, to the *cyclin D1* promoter in *Cyld*$^{-/-}$ keratinocytes (Figure 5J). These data supports a model in which TPA or UV-B treatment leads to the translocation of Cyld to the perinuclear region, where Cyld binds Bcl-3 and inhibits its nuclear accumulation. In the absence of Cyld, however, Bcl-3 accumulates in the nucleus and forms a complex with p50 or p52 that is recruited to the NF-κB site in the *cyclin D1* promoter.

Depletion of Bcl-3 in *Cyld*$^{-/-}$ Keratinocytes Reduces TPA-Induced *cyclin D1* Promoter Activity and Proliferation

If the increased nuclear accumulation of Bcl-3 and the elevated binding to the NF-κB binding site of the *cyclin D1* promoter are indeed directly responsible for the enhanced cyclin D1 expression and proliferation of *Cyld*$^{-/-}$

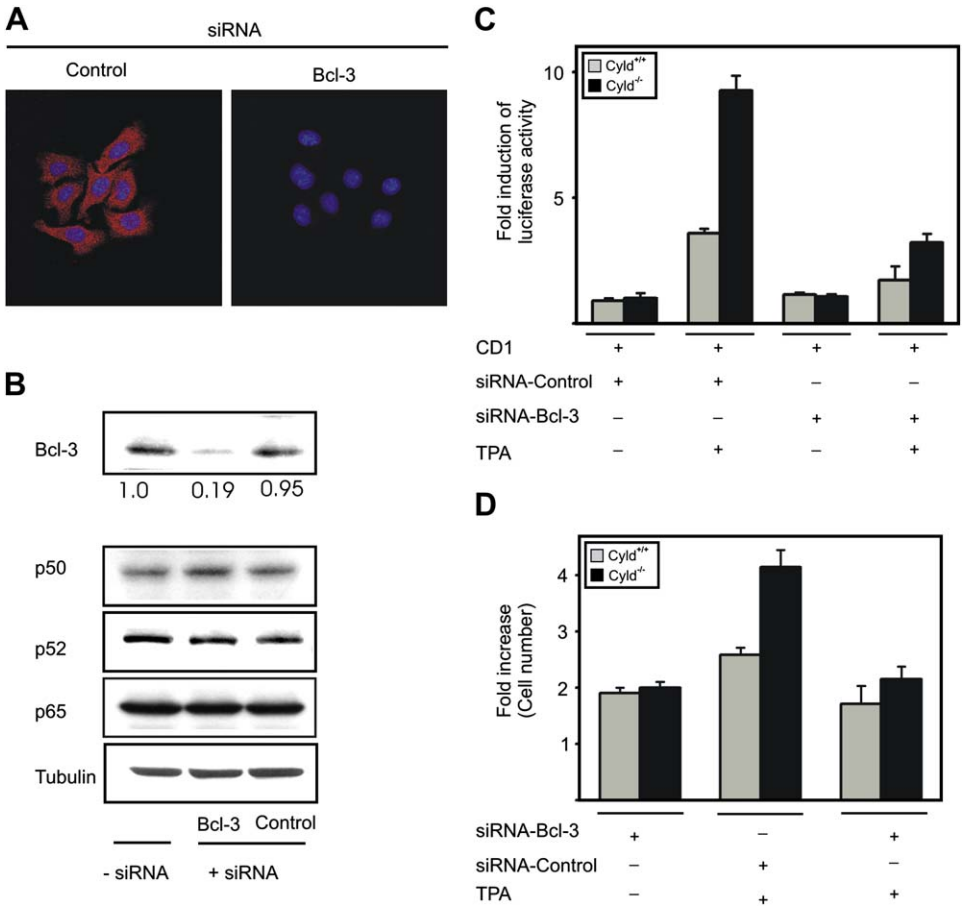

Figure 6. siRNA-Induced Knockdown of Bcl-3 in Keratinocytes

(A) Confocal plane of Bcl-3 (red) and DAPI (blue) in control- or Bcl-3 siRNA-transfected *Cyld*$^{-/-}$ keratinocytes.

(B) Western blot analysis of Bcl-3, p50, p52, and p65 proteins in *Cyld*$^{-/-}$ keratinocytes before or after transfection with Bcl-3 siRNA. Numbers indicate the ratio of Bcl-3 protein in nontransfected cells versus siRNA-transfected cells.

(C) Activation of the *cyclin D1* promoter luciferase reporter in *Cyld*$^{+/+}$ and *Cyld*$^{-/-}$ keratinocytes cotransfected with control or Bcl-3-specific siRNA in the absence or presence of TPA (100 nM; 2 hr). Transfection of Bcl-3 siRNA significantly reduced TPA-induced *cyclin D1* activity when compared to control siRNA ($n = 4$; $p < 0.05$).

(D) Cell proliferation assay of *Cyld*$^{+/+}$ and *Cyld*$^{-/-}$ keratinocytes cotransfected with control or Bcl-3-specific siRNA in the absence or presence of TPA (100 nM). The proliferation rate after 48 hr is significantly reduced upon Bcl-3 siRNA transfection ($n = 6$; $p < 0.05$).

keratinocytes, depletion of Bcl-3 should reverse the phenotype. We therefore used small interfering RNA (siRNA) to deplete Bcl-3 expression in *Cyld*$^{+/+}$ and *Cyld*$^{-/-}$ keratinocytes (Figures 6A and 6B), which had no apparent impact on the levels of NF-κB p50, p52, and p65 (Figures 6B). Depletion of Bcl-3 significantly reduced TPA-induced *cyclin D1* promoter activation in both *Cyld*$^{-/-}$ and *Cyld*$^{+/+}$ keratinocytes. Treatment of keratinocytes with control siRNA unrelated to any known genes did not affect *cyclin D1* activity (Figure 6C). Similarly, depletion of Bcl-3 also reversed the increased proliferation rate of *Cyld*$^{-/-}$ keratinocytes, while treatment with control siRNA had no effect (Figure 6D). These findings indicate that Bcl-3 is required for the inhibitory effect of Cyld on TPA- and UV-induced *cyclin D1* activation and proliferation.

Cyld-Mediated Deubiquitination of Bcl-3 Prevents Accumulation of Bcl-3 in the Nucleus

To test whether the retention of Bcl-3 is dependent on the deubiquitinating activity of Cyld, we immunoprecipitated endogenous Bcl-3 in untreated and TPA-treated *Cyld*$^{+/+}$ and *Cyld*$^{-/-}$ keratinocytes and subsequently determined the modification of Bcl-3 with ubiquitin. The polyubiquitination of Bcl-3 in untreated *Cyld*$^{+/+}$ and *Cyld*$^{-/-}$ keratinocytes was weak and similar between the two cell types. While TPA stimulation failed to increase the polyubiquitination of Bcl-3 in *Cyld*$^{+/+}$ keratinocytes, it caused significant polyubiquitination of Bcl-3 in *Cyld*$^{-/-}$ keratinocytes 30 min after TPA addition, which further increased within 60 min (Figure 7A). In order to determine the type of polyubiquitin chains that Cyld removes from Bcl-3 in vivo, we

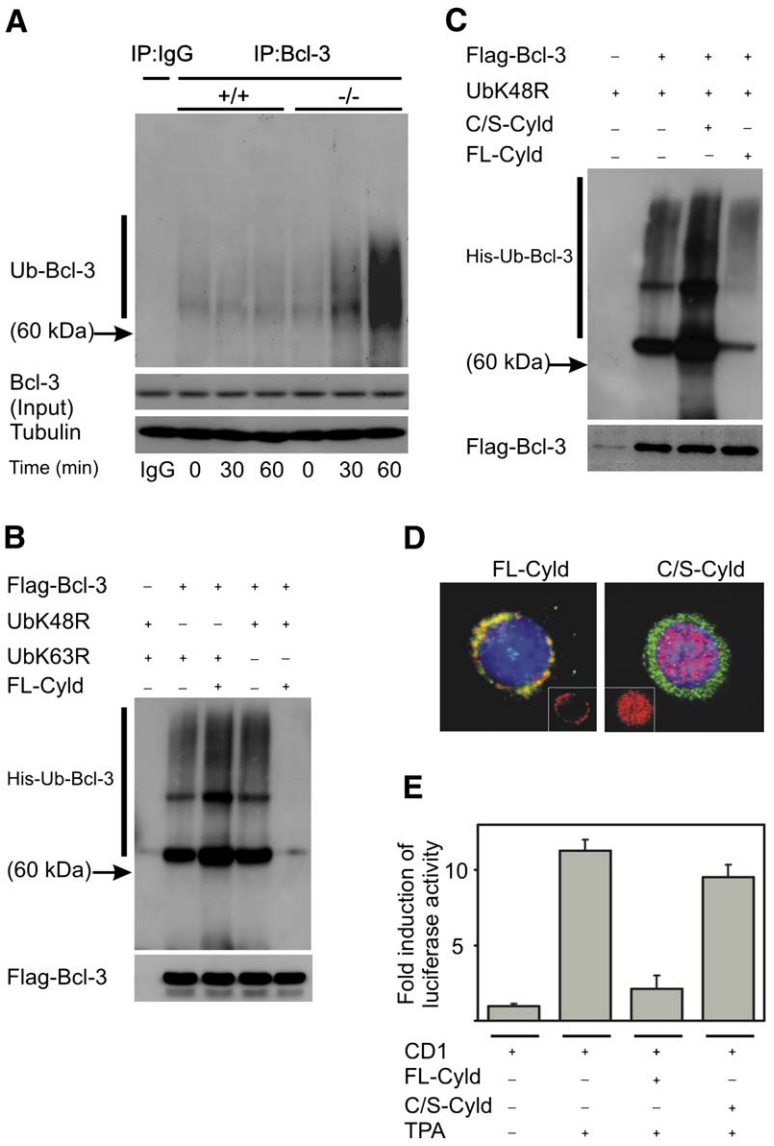

Figure 7. Deubiquitination of Bcl-3 by Cyld

(A) Endogenous ubiquitination of Bcl-3 using *Cyld*$^{+/+}$ and *Cyld*$^{-/-}$ keratinocytes in the presence or absence of TPA. The top panel shows immunoprecipitation with antibodies directed against Bcl-3 or control antibodies (preimmune serum; IgG). Immunoprecipitates were resolved on an SDS gel and probed with anti-ubiquitin antibodies. The middle panel shows that equal amounts of Bcl-3 were used for immunoprecipitation. The lower panel shows cell lysate probed with anti-tubulin antibody.

(B) HeLa cells were transfected with mutant His-tagged ubiquitin cDNAs, Flag-tagged Bcl-3, and full-length wild-type Cyld (FL-Cyld). Bcl-3 was immunoprecipitated with an anti-Flag (M2) antibody and then immunoblotted with antisera against ubiquitin, stripped, and reprobed with an antibody against Flag.

(C) Ubiquitination of Bcl-3 was carried out as in (B) in the presence of the ubiquitin mutants and with either full-length wild-type Cyld (FL-Cyld) or enzymatically inactive Cyld (C/S-Cyld) as indicated.

(D) Confocal plane of TPA-stimulated (30 min) *Cyld*$^{-/-}$ keratinocytes transduced with FL-Cyld (green) or C/S-Cyld (green) and immunostained for Bcl-3 (red). Inserts show Bcl-3 localization only.

(E) Activation of the −64 to +10 *cyclin D1* promoter luciferase reporter construct with the κB site in *Cyld*$^{-/-}$ (CD1), FL-Cyld, or C/S mutant stably transfected keratinocytes in the absence or presence of TPA (100 nM, 2 hr). The *cyclin D1* activity in TPA-treated FL-Cyld keratinocytes compared to C/S mutant is significantly different ($n = 5$; $p < 0.05$).

performed ubiquitination assays using specific point mutants of His-tagged ubiquitin in which either K48 or K63 is replaced by an arginine (UbK48R and UbK63R). While Cyld removed UbK48R from Bcl-3 very efficiently, Cyld was unable to remove UbK63R (Figure 7B). Altogether, these findings indicate that Cyld catalyzes the disassembly of K63-linked rather than K48-linked polyubiquitin chains on Bcl-3 in vivo.

To further test the importance of the deubiquitinase activity of Cyld for nuclear accumulation and function of Bcl-3, we rescued *Cyld*$^{-/-}$ keratinocytes with full-length Cyld (FL-Cyld) and a Cyld cDNA that carries a point mutation in the cysteine box of the deubiquitinase domain (C/S-Cyld; Brummelkamp et al., 2003). Expression of the C/S-Cyld in *Cyld*$^{-/-}$ keratinocytes was indeed unable to remove K63-linked ubiquitin chains from Bcl-3 (Figure 7C). To test whether C/S-Cyld is able to reverse the cyclin D1 hyperactivation and proliferation of *Cyld*$^{-/-}$ keratinocytes, we expressed the catalytically inactive mutant or the wild-type form of full-length Cyld in *Cyld*$^{-/-}$ keratinocytes. As expected, wild-type Cyld efficiently inhibited TPA- or UV-B-induced nuclear accumulation of Bcl-3, while the catalytically inactive mutant of Cyld was unable to prevent nuclear accumulation of Bcl-3 (Figure 7D) and activation of the *cyclin D1* promoter (Figure 7E). Based on these data, we conclude that Cyld binds to and removes lysine 63-linked ubiquitin chains from Bcl-3 in TPA- or UV-B-treated keratinocytes and that deubiquitination prevents Bcl-3 accumulation in the nucleus and activation of the *cyclin D1* promoter (Figure 8).

DISCUSSION

Mutations in the tumor suppressor gene *CYLD* cause benign tumors called cylindromas that are believed to

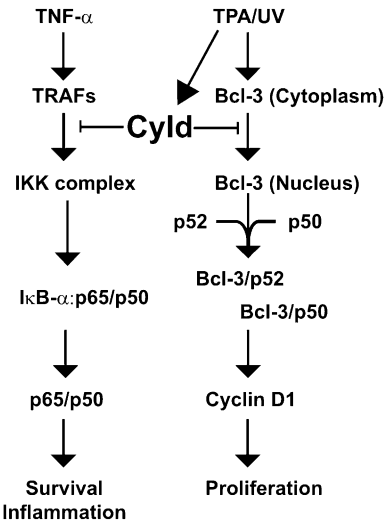

Figure 8. Model of How Cyld Regulates TNF-α- or TPA/UV-Induced NF-κB Signaling in Keratinocytes

develop from hair-follicle keratinocytes (Bignell et al., 2000). In the search for the tumor suppressor function of CYLD, several laboratories reported that CYLD can inhibit the activation of the classical NF-κB p65/p50 transcription factor (Trompouki et al., 2003; Brummelkamp et al., 2003; Kovalenko et al., 2003; Regamey et al., 2003). While hyperactivation of NF-κB p65/p50 promotes cell survival and/or cell proliferation in most cell types (Karin et al., 2002), keratinocytes respond with growth arrest and terminal differentiation (Seitz et al., 1998), pointing to the possibility that additional signaling pathways may be affected in Cyld-deficient tumor cells. In the present paper, we tested this hypothesis by analyzing skin tumor formation in mice lacking Cyld.

Cyld-deficient mice developed and aged normally despite the ubiquitous expression pattern of Cyld. When we induced tumors with DMBA and TPA in Cyld-deficient mice, we found that they suffered from a significantly higher tumor incidence and developed significantly larger and more tumors than their littermate controls. The increased tumor development in Cyld-deficient mice was due to a dramatically elevated tumor cell proliferation, while tumor cell survival was not significantly altered. In search of a mechanistic explanation for the dysregulated proliferation rate in Cyld-deficient tumors, we identified several steps of a signaling pathway in which Cyld undertakes the principal task of controlling the nuclear translocation of Bcl-3, which in turn alters the transcriptional properties of the NF-κB p50 and p52 homodimers. Growth-promoting signals such as TPA or UV light trigger the translocation of Cyld and Bcl-3 from the cytoplasm to the perinuclear region. Following this translocation, Cyld removes K63-linked polyubiquitin chains from Bcl-3, which prevents Bcl-3 from translocating into the nucleus. In support of these findings, we observed that loss of Cyld or the expression of a catalytically inactive *Cyld* mutant failed to deubiquitinate the perinuclear Bcl-3, which in turn facilitated the nuclear accumulation of Bcl-3. Nuclear Bcl-3 associated with p50 and p52 at NF-κB binding sites and activated transcription of NF-κB target genes such as *cyclin D1*. Importantly, the same signaling pathway described here for mouse epidermal keratinocytes also operates in human cylindromas, which are believed to develop from hair follicles. Immunostaining of tumor sections from cylindroma patients revealed that the majority of tumor cells contained Bcl-3 in the nucleus, while epidermal or hair-follicle keratinocytes of normal human skin retained Bcl-3 in the cytoplasm, strongly suggesting that CYLD also controls Bcl-3 translocation into the nucleus of hair-follicle keratinocytes.

Our findings show that the cytoplasmic Bcl-3 is inactive and requires lysine 63 polyubiquitination in order to translocate into the nucleus. The polyubiquitin modification of Bcl-3 could facilitate the interaction with nuclear transport receptors (called importins) and mediate the transport through the nuclear core complex, as shown for the monoubiquitinated E2 conjugating enzyme UbcM2 (Plafker et al., 2004). It is also conceivable, however, that the polyubiquitin chains of Bcl-3 enable binding to nuclear proteins with the consequence that such interactions target Bcl-3 to a specific nuclear compartment. Nuclear Bcl-3 was shown to associate with p50 and p52 in a large number of different tumor cell lines and to promote cell proliferation and oncogenesis through the activation of the *cyclin D1* gene (Cogswell et al., 2000; Thornburg et al., 2003; Budunova et al., 1999). In light of our current findings, it will be important to determine whether the increased nuclear Bcl-3 levels in these tumor cell lines are (like in cylindromas and epidermal tumors) also caused by absent or decreased Cyld expression.

Since most tumors in our mouse model develop from epidermal keratinocytes rather than from hair-follicle keratinocytes, we began to determine the CYLD levels in human skin tumors such as basal cell carcinomas (BCC) and squamous cell carcinomas (SCC) that also develop from epidermal keratinocytes. Interestingly, we observed reduced or absent expression of CYLD in more than ten samples of BCC and SCC, respectively (R.M., unpublished data). This strongly suggests that CYLD plays a general role as a tumor suppressor, which is in agreement with its ubiquitous expression pattern and with a recent observation showing that CYLD levels are downregulated in several other tumors such as kidney, liver, and uterine cervix (Strobel et al., 2002; Hashimoto et al., 2004; Hirai et al., 2004).

Although TNF-α-induced signaling via TRAF2-dependent p65/p50 activation is enhanced in Cyld-deficient keratinocytes, the significance of this pathway for the development of tumors is not clear. On one hand, overexpression of NF-κB p65/p50 stimulated neither the basal nor the TPA-induced proliferation rate of Cyld-deficient keratinocytes, suggesting that the classical NF-κB signaling pathway is not contributing to the exacerbation of tumor cell proliferation in Cyld-deficient tumors. On the

other hand, we found no compelling evidence for an enhanced survival of tumor cells in Cyld-deficient mice. It is possible, however, that NF-κB dependent p65/p50 signaling becomes crucial when cylindroma tumors reach a certain size and erode, leading to bacterial superinfection. In such situations, pathogens and cytokines may activate NF-κB p65/p50 signaling through Toll-like receptors and cytokine receptors, which are expressed on keratinocytes (Mempel et al., 2003; Kollisch et al., 2005), and may then promote survival of tumor cells and contribute to the growth of Cyld-deficient tumors. If so, the mode of stimulation may dictate whether Cyld controls inflammation through TRAF signaling and p65/p50 activation (Figure 8) or tumor growth through Bcl-3 activation, NF-κB p50 and/or p52 binding, and, finally, activation of NF-κB-dependent gene transcription.

EXPERIMENTAL PROCEDURES

Generation of *Cyld*$^{-/-}$ Mice and Genotyping

Cyld$^{-/-}$ mice were generated with a targeting construct in which the ATG-containing exon 4 of the *Cyld* gene was disrupted with a *lacZ* reporter and a *neomycin* gene. The targeting vector was electroporated into R1 embryonic stem (ES) cells (passage 13), and two independently targeted ES cell clones were injected into C57Bl/6 blastocysts to generate germline chimeras. The chimeric founders were crossed to C57Bl/6 females to establish heterozygous *Cyld*$^{+/-}$ and subsequently homozygous *Cyld*$^{-/-}$ mice. Fifth-generation backcrosses into C57Bl/6 were used for the chemically induced tumor experiments.

Sections of mouse tumor tissues or cylindromas from three patients were fixed with 3% PFA, paraffin embedded, and stained with an affinity-purified rabbit anti-mouse Cyld antiserum or a rabbit anti-Bcl-3 antiserum.

Carcinogenesis Protocols

For two-stage chemical carcinogenesis, cohorts of 8-week-old sex-matched *Cyld*$^{+/+}$, *Cyld*$^{+/-}$, and *Cyld*$^{-/-}$ littermates backcrossed five times to C57Bl/6 were treated for 1 week with DMBA (25 μg in 200 μl acetone) and then for 16 weeks with TPA (200 μl of 10^{-4} M solution in acetone). For complete carcinogenesis, mice were treated biweekly with 5 μg DMBA alone in 200 μl acetone for 21 weeks. Tumors and organs were snap frozen in liquid nitrogen, fixed in formalin, and stained with hematoxylin and eosin or antisera against Cyld (generated by immunizing rabbits with a bacterially expressed GST-fusion protein with the N-terminal 323 amino acids of mouse Cyld), BrdU (DAKO), Ki-67 (Novocastra), or cyclin D1 (Santa Cruz). Secondary antibodies were purchased from Jackson Laboratories.

Cell Proliferation and Apoptosis in Skin

Cohorts of *Cyld*$^{+/+}$ and *Cyld*$^{-/-}$ littermates were treated with a single application of TPA alone, injected intraperitoneally with BrdU (100 mg/kg; Sigma) 48 hr later, and then killed 3 hr later. Cell proliferation was determined in skin sections using antibodies against BrdU (DAKO), Ki67 antigen (Novocastra), or cyclin D1 (Santa Cruz). Apoptosis was determined by immunostaining for cleaved caspase-3 (Cell Signaling) or visualizing TUNEL (TdT-mediated dUTP nick end labeling) positive cells. The percentage of signal-positive keratinocytes in the basal layer of interfollicular epidermis was calculated from ten different fields of at least five different tumors.

Primary Keratinocyte Culture, Transfection, and Reporter Assays

Primary keratinocytes were isolated from back skin of 8-week-old mice and cultured as described (Romero et al., 1999). The p50, p52, p65, and Bcl-3 expression constructs and the −64 to +10 *cyclin D1* promoter luciferase reporter construct with (pCD1) and without (Mut-CD1) the NF-κB binding were used for the luciferase activation assay. HA-tagged Cyld was PCR amplified and cloned into pCS2 vector. Cell transfection assays were carried out in six-well plates at 80% confluence with Polyfectamine (QIAGEN) according to the manufacturer's instructions. All cell transfection assays were repeated between four and six times (as indicated) and were always done in triplicate. To assay for transfection efficiency, transfections were done with a constant amount of a Renilla expression plasmid. Luciferase and Renilla activities were assayed 24 hr after transfection according to the manufacturer's instructions (Promega). TPA or TNF-α (both purchased from Sigma) stimulation was done for 2 hr. Stable expression of Cyld was achieved by retro- or lentiviral infection (Pfeifer et al., 2000). siRNAs (control and Bcl-3) were purchased from Santa Cruz and used according to the manufacturer's instructions. siRNA transfections were made with HiPerFect transfection reagent (QIAGEN).

Immunoblots, Immunoprecipitation, and Chromatin Immunoprecipitation

For immunoblotting, lysates from whole cells and cytosolic and nuclear extracts were resolved in SDS-PAGE gels, transferred to PVDF membranes, and incubated with the following antibodies: anti-SAPK/JNK, anti-phospho-p38 MAP kinase, anti-phospho-Akt, anti-phospho-SAPK/JNK, anti-p38 MAP kinase, anti-phospho-IκB-α, and anti-Akt (all from Cell Signaling); anti-IκB-α (c-21), anti-p65, anti-p50, anti-ubiquitin, and anti-Bcl-3 (from Santa Cruz); and anti-p52 (from Abcam).

For immunoprecipitations, lysates were obtained from untreated or TPA-treated (100 nM TPA for different time periods: 15, 30, 60, or 90 min) primary keratinocytes. The samples were centrifuged at 10,000 × g for 20 min. For anti-Bcl-3 immunoprecipitation, the lysates were precleared for 30 min at 4°C. The protein content was determined and compensated for equal content in all supernatants. For testing protein input, a small part of the resulting lysates was gel separated and immunoblotted (Bcl-3 protein input, Figure 7A), and the remaining part was used for immunoprecipitation. Immunoblots were developed with the ECL-plus reagent (Amersham Biosciences) according to the manufacturer's instructions.

Chromatin immunoprecipitation (ChIP) was performed according to the manufacturer's instructions (Imgenex Corporation) using either Bcl-3 (Santa Cruz); p50, p52, or p50 antibodies; or rabbit IgG. The extracted DNA was used for semiquantitative PCR to amplify the *cyclin D1* promoter region.

Two-Hybrid and Galactosidase Assays

Cyld and Bcl-3 cDNAs were cloned as bait and prey in pGBKT7 (BD) and pGADT7 (AD) (Clontech), respectively. Two-hybrid interaction analyses were done using the Matchmaker Two-Hybrid System (Clontech) according to the manufacturer's instructions. In brief, after selection of cotransformants, the interaction of fusion proteins was detected on high-stringency plates (SD/−Ade/−His/−Leu/−Trp) and verified by β-galactosidase filter assays.

Statistical Analysis

Values are presented as the means ± SEM, with n indicating the number of independent experiments. Statistical differences were determined using Student's t test.

Supplemental Data

Supplemental Data include eight figures and can be found with this article online at http://www.cell.com/cgi/content/full/125/4/665/DC1/.

ACKNOWLEDGMENTS

We thank Michael Boesl and the MPI transgenic service for the generation of *Cyld*$^{-/-}$ mice; Heidi Sebald for expert technical assistance; Drs. Ralf Paus, Nils Cordes, Erik Danen, Arnoud Sonnenberg, and

Kyle Legate for discussion and critical reading of the manuscript; Attila Braun and Bodo Haas for help with cloning; Drs. Ludger Hengst, Roland Schmid, Martin Eilers, and René Bernards for plasmid gifts; and Maurizio Podda for cylindroma and human skin samples. R.M. received fellowships from the Swedish Cancer Foundation and the Tegger Foundation. This work was supported by the Max Planck Society, Fonds der Chemischen Industrie, and the DFG to R.F.

Received: December 4, 2005
Revised: January 31, 2006
Accepted: March 3, 2006
Published: May 18, 2006

REFERENCES

Bignell, G.R., Warren, W., Seal, S., Takahashi, M., Rapley, E., Barfoot, R., Green, H., Brown, C., Biggs, P.J., Lakhani, S.R., et al. (2000). Identification of the familial cylindromatosis tumour-suppressor gene. Nat. Genet. *25*, 160–165.

Bours, V., Franzoso, G., Azarenko, V., Park, S., Kanno, T., Brown, K., and Siebenlist, U. (1993). The oncoprotein Bcl-3 directly transactivates through kappa B motifs via association with DNA-binding p50B homodimers. Cell *72*, 729–739.

Brasier, A.R., Lu, M., Hai, T., Lu, Y., and Boldogh, I. (2001). NF-kappa B-inducible BCL-3 expression is an autoregulatory loop controlling nuclear p50/NF-kappa B1 residence. J. Biol. Chem. *276*, 32080–32093.

Brummelkamp, T.R., Nijman, S.M., Dirac, A.M., and Bernards, R. (2003). Loss of the cylindromatosis tumour suppressor inhibits apoptosis by activating NF-κB. Nature *424*, 797–801.

Budunova, I.V., Perez, P., Vaden, V.R., Spiegelman, V.S., Slaga, T.J., and Jorcano, J.L. (1999). Increased expression of p50-NF-κB and constitutive activation of NF-κB transcription factors during mouse skin carcinogenesis. Oncogene *18*, 7423–7431.

Cogswell, P.C., Guttridge, D.C., Funkhouser, W.K., and Baldwin, A.S., Jr. (2000). Selective activation of NF-κB subunits in human breast cancer: potential roles for NF-κB2/p52 and for Bcl-3. Oncogene *19*, 1123–1131.

Fujita, T., Nolan, G.P., Liou, H.C., Scott, M.L., and Baltimore, D. (1993). The candidate proto-oncogene bcl-3 encodes a transcriptional coactivator that activates through NF-κB p50 homodimers. Genes Dev. *7*, 1354–1363.

Ghosh, S., and Karin, M. (2002). Missing pieces in the NF-κB puzzle. Cell *109*, 81–96.

Guttridge, D.C., Albanese, C., Reuther, J.Y., Pestell, R.G., and Baldwin, A.S., Jr. (1999). NF-κB controls cell growth and differentiation through transcriptional regulation of cyclin D1. Mol. Cell. Biol. *19*, 5785–5799.

Hashimoto, K., Mori, N., Tamesa, T., Okada, T., Kawauchi, S., Oga, A., Furuya, T., Tangoku, A., Oka, M., and Sasaki, K. (2004). Analysis of DNA copy number aberrations in hepatitis C virus-associated hepatocellular carcinomas by conventional CGH and array CGH. Mod. Pathol. *17*, 617–622.

Hinz, M., and Strauss, M. (1999). NF-κB function in growth control: regulation of cyclin D1 expression and G0/G1-to-S-phase transition. Mol. Cell. Biol. *19*, 2690–2698.

Hirai, Y., Kawamata, Y., Takeshima, N., Furuta, R., Kitagawa, T., Kawaguchi, T., Hasumi, K., Sugai, S., and Noda, T. (2004). Conventional and array-based comparative genomic hybridization analyses of novel cell lines harboring HPV18 from glassy cell carcinoma of the uterine cervix. Int. J. Oncol. *24*, 977–986.

Israel, A. (2000). The IKK complex: an integrator of all signals that activate NF-κB? Trends Cell Biol. *10*, 129–133.

Joyce, D., Albanese, C., Steer, J., Fu, M., Bouzahzah, B., and Pestell, R.G. (2001). NF-κB and cell-cycle regulation: the cyclin connection. Cytokine Growth Factor Rev. *1*, 73–90.

Karin, M., Cao, Y., Greten, F.R., and Li, Z.W. (2002). NF-κB in cancer: from innocent bystander to major culprit. Nat. Rev. Cancer *2*, 301–310.

Kollisch, G., Kalali, B.N., Voelcker, V., Wallich, R., Behrendt, H., Ring, J., Bauer, S., Jakob, T., Mempel, M., and Ollert, M. (2005). Various members of the Toll-like receptor family contribute to the innate immune response of human epidermal keratinocytes. Immunology *114*, 531–541.

Kovalenko, A., Chable-Bessia, C., Cantarella, G., Israel, A., Wallach, D., and Courtois, G. (2003). The tumour suppressor CYLD negatively regulates NF-κB signalling by deubiquitination. Nature *424*, 801–805.

Liang, J., and Slingerland, J.M. (2003). Multiple roles of the PI3K/PKB (Akt) pathway in cell cycle progression. Cell Cycle *4*, 339–345.

McKeithan, T.W., Ohno, H., and Diaz, M.O. (1990). Identification of a transcriptional unit adjacent to the breakpoint in the 14;19 translocation of chronic lymphocytic leukemia. Genes Chromosomes Cancer *1*, 247–255.

Mempel, M., Voelcker, V., Kollisch, G., Plank, C., Rad, R., Gerhard, M., Schnopp, C., Fraunberger, P., Walli, A.K., Ring, J., et al. (2003). Toll-like receptor expression in human keratinocytes: nuclear factor kappaB controlled gene activation by Staphylococcus aureus is toll-like receptor 2 but not toll-like receptor 4 or platelet activating factor receptor dependent. J. Invest. Dermatol. *121*, 1389–1396.

Nishikori, M., Maesako, Y., Ueda, C., Kurata, M., Uchiyama, T., and Ohno, H. (2003). High-level expression of BCL3 differentiates t(2;5)(p23;q35)-positive anaplastic large cell lymphoma from Hodgkin disease. Blood *101*, 2789–2796.

Nolan, G.P., Fujita, T., Bhatia, K., Huppi, C., Liou, H.C., Scott, M.L., and Baltimore, D. (1993). The bcl-3 proto-oncogene encodes a nuclear I kappa B-like molecule that preferentially interacts with NF-kappa B p50 and p52 in a phosphorylation-dependent manner. Mol. Cell. Biol. *13*, 3557–3566.

Pfeifer, A., Kessler, T., Silletti, S., Cheresh, D.A., and Verma, I.M. (2000). Suppression of angiogenesis by lentiviral delivery of PEX, a noncatalytic fragment of matrix metalloproteinase 2. Proc. Natl. Acad. Sci. USA *97*, 12227–12232.

Pickart, C.M. (2001). Mechanisms underlying ubiquitination. Annu. Rev. Biochem. *70*, 503–533.

Plafker, S.M., Plafker, K.S., Weissman, A.M., and Macara, I.G. (2004). Ubiquitin charging of human class III ubiquitin-conjugating enzymes triggers their nuclear import. J. Cell Biol. *167*, 649–659.

Quintanilla, M., Brown, K., Ramsden, M., and Balmain, A. (1986). Carcinogen-specific mutation and amplification of Ha-ras during mouse skin carcinogenesis. Nature *322*, 78–80.

Regamey, A., Hohl, D., Liu, J.W., Roger, T., Kogerman, P., Toftgard, R., and Huber, M. (2003). The tumor suppressor CYLD interacts with TRIP and regulates negatively nuclear factor kappaB activation by tumor necrosis factor. J. Exp. Med. *198*, 1959–1964.

Rocha, S., Martin, A.M., Meek, D.W., and Perkins, N.D. (2003). p53 represses cyclin D1 transcription through down regulation of Bcl-3 and inducing increased association of the p52 NF-κB subunit with histone deacetylase 1. Mol. Cell. Biol. *23*, 4713–4727.

Romero, M.R., Carroll, J.M., and Watt, F.M. (1999). Analysis of cultured keratinocytes from a transgenic mouse model of psoriasis: effects of suprabasal integrin expression on keratinocyte adhesion, proliferation and terminal differentiation. Exp. Dermatol. *8*, 53–67.

Seitz, C.S., Lin, Q., Deng, H., and Khavari, P.A. (1998). Alterations in NF-κB function in transgenic epithelial tissue demonstrate a growth inhibitory role for NF-κB. Proc. Natl. Acad. Sci. USA *95*, 2307–2312.

Strobel, P., Zettl, A., Ren, Z., Starostik, P., Riedmiller, H., Storkel, S., Muller-Hermelink, H.K., and Marx, A. (2002). Spiradenocylindroma of

the kidney: clinical and genetic findings suggesting a role of somatic mutation of the CYLD1 gene in the oncogenesis of an unusual renal neoplasm. Am. J. Surg. Pathol. *26*, 119–124.

Thornburg, N.J., Pathmanathan, R., and Raab-Traub, N. (2003). Activation of nuclear factor-κB p50 homodimer/Bcl-3 complexes in nasopharyngeal carcinoma. Cancer Res. *63*, 8293–8301.

Trompouki, E., Hatzivassiliou, E., Tsichritzis, T., Farmer, H., Ashworth, A., and Mosialos, G. (2003). CYLD is a deubiquitinating enzyme that negatively regulates NF-κB activation by TNFR family members. Nature *424*, 793–796.

van Balkom, I.D., and Hennekam, R.C. (1994). Dermal eccrine cylindromatosis. J. Med. Genet. *31*, 321–324.

Watanabe, N., Iwamura, T., Shinoda, T., and Fu, T. (1997). Regulation of NFKB1 proteins by the candidate oncoprotein BCL-3: generation of NF-κB homodimers from the cytoplasmic pool of p50–p105 and nuclear translocation. EMBO J. *16*, 3609–3620.

Weissman, A.M. (2001). Themes and variations on ubiquitylation. Nat. Rev. Mol. Cell Biol. *2*, 169–178.

Westerheide, S.D., Mayo, M.W., Anest, V., Hanson, J.L., and Baldwin, A.S., Jr. (2001). The putative oncoprotein Bcl-3 induces cyclin D1 to stimulate G(1) transition. Mol. Cell. Biol. *21*, 8428–8436.

Wilkinson, M.G., and Millar, J.B. (2000). Control of the eukaryotic cell cycle by MAP kinase signaling pathways. FASEB J. *14*, 2147–2157.

Zhang, M.Y., Harhaj, E.W., Bell, L., Sun, S.C., and Miller, B.A. (1998). Bcl-3 expression and nuclear translocation are induced by granulocyte-macrophage colony-stimulating factor and erythropoietin in proliferating human erythroid precursors. Blood *92*, 1225–1234.

Zhang, Q., Didonato, J.A., Karin, M., and McKeithan, T.W. (1994). BCL3 encodes a nuclear protein which can alter the subcellular location of NF-kappa B proteins. Mol. Cell. Biol. *14*, 3915–3926.